



Cite this: *Soft Matter*, 2020, **16**, 1333

Archaeal cyclopentane fragment in a surfactant's hydrophobic tail decreases the Krafft point

Konstantin S. Mineev,^{ab} Pavel E. Volynsky,^a Timur R. Galimzyanov,^{cd} Daria S. Tretiakova,^{ac} Mikhail Y. Bobrov,^{ae} Anna S. Alekseeva^{ac} and Ivan A. Boldyrev^{id,*acf}

Archaea are prokaryotic microorganisms famous for their ability to adapt to extreme environments, including low and high temperatures. Archaeal lipids often are macrocycles with two polar heads and a hydrophobic core that contains methyl groups and in-line cycles. Here we present the design of novel general-purpose surfactants that have inherited features of archaeal lipids. These are C12 and C14 carboxylic acids containing in-line cyclopentanes. The cyclopentanes disturb the chain packing, which results in remarkable expansion of the operational range of the surfactant into the low-temperature region. We report synthesis and properties of these novel archaea-like surfactants and details of their chain packing derived from thermodynamics model predictions, molecular dynamics simulations, and experimental data on CMC and Krafft points.

Received 7th October 2019,
Accepted 19th December 2019

DOI: 10.1039/c9sm02000d

rsc.li/soft-matter-journal

Introduction

Archaea are prokaryotic microbes that are known to adapt to extreme environments such as low and high temperatures (as high as over 100 °C, at which they are found in geysers and black smokers), ultra-low or ultra-high pH (pH < 1 or pH > 11), high pressure and high salinity. Numerous efforts have been made to apply the unique features of archaea in modern bio- and nanotechnology. The incomplete list of recent achievements includes the use of archaea in industrial biomineralization,^{1,2} wastewater treatment,^{3,4} and the production of biogas.⁵ The industrial future of archaeal enzymes and proteins has already begun (see recent reviews^{6–8} and exciting reports on metal bioremediation,⁹ carotenoid isolation,¹⁰ and ethanol production¹¹). The progress in the utilization of archaeal lipids is slower, although they have great industrial prospects as materials for lightweight self-assembling films and coatings that are resistant to extreme environments. The progress in the development of archaea-like surface-active compounds is impeded because of the very complex structure of archaeal lipids. Many of these lipids are macrocycles with two polar

heads and a hydrophobic core that contains methyl groups and in-line cycles¹² (Fig. 1A). The role of the in-line cycles has been thoroughly investigated.^{13–21} It is assumed that the role of in-line cyclopentane fragments should be similar to that of in-line double bonds in conventional lipids: they introduce kinks in hydrophobic chains and thereby cause chain disordering. But in contrast to double bonds, cyclopentane fragments are chemically stable.

Here, we investigate general-purpose surfactants that inherit features of archaeal lipids. These surfactants are single chain, single polar head molecules with in-line cyclopentanes, which disturb the chain packing (Fig. 1).

Experimental

Starting compounds and silica were obtained from Merck KGaA (Darmstadt, Germany). Solvents were obtained from Ekos-1 (Moscow, Russia). Structures of the obtained compounds were confirmed by the conventional heteronuclear NMR approach. For this purpose, a set of 2D NMR spectra obtained from multiplicity-edited ¹H, ¹³C-HSQC,²² DQF-COSY, ¹H, ¹³C-HMBC and several ¹H, ¹³C-HSQC-TOCSY experiments performed at different mixing times (10, 20, 40 and 60 ms; DIPSI-2 mixing) were recorded on a Bruker Avance 700 MHz NMR spectrometer.

Configurations of the obtained compounds were determined based on the NOE analysis and vicinal proton–proton J-couplings. The NOESY spectra were recorded at 30 °C using a mixing time of 400 ms; zero-quantum coherence was

^a Shemyakin-Ovchinnikov Institute of Bioorganic Chemistry, Russian Academy of Sciences, Moscow, 117997, Russia. E-mail: ivan@lipids.ibch.ru

^b Moscow Institute of Physics and Technology, Dolgoprudnyi, 141700, Russia

^c National University of Science and Technology MISiS, Moscow, 119049, Russia

^d Frumkin Institute of Physical Chemistry and Electrochemistry, Russian Academy of Sciences, Moscow, 119071, Russia

^e Scientific Centre for Obstetrics, Gynaecology and Perinatology, Ministry of Healthcare of Russian Federation, Moscow, 117997, Russia

^f Pirogov Russian National Research Medical University, Moscow, 117997, Russia

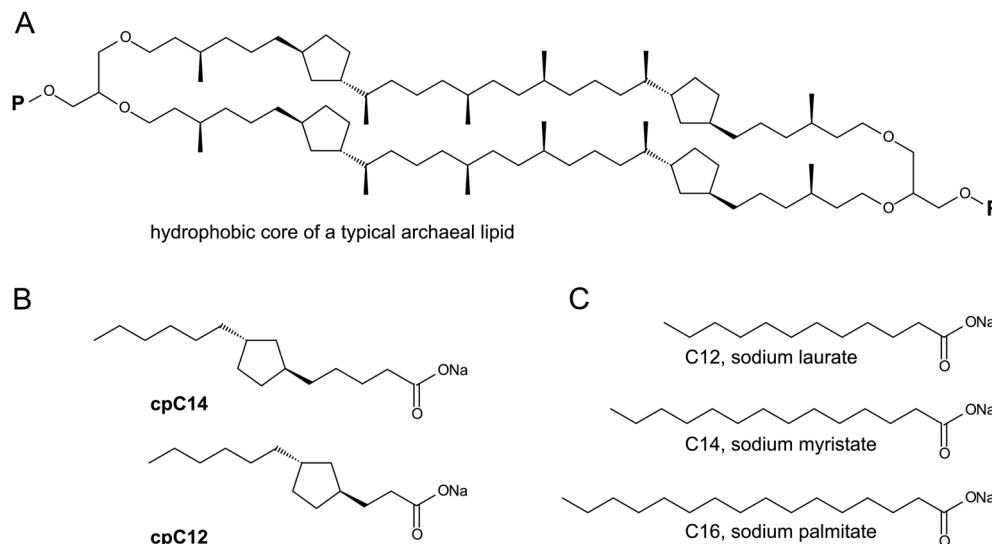


Fig. 1 (A) Many of archaeal lipids are macrocycles that bear two polar heads (marked with P) and contain methyl groups and in-line cycles in the hydrophobic core. (B) Cyclopentane-containing surfactants used in this study. (C) Common surfactants used in this study as reference substances.

suppressed by using a Z-gradient pulse and a swept-frequency adiabatic pulse simultaneously.²³ Vicinal *J*-couplings were measured by the deconvolution of well-resolved multiplets using the Wolfram Mathematica 8.0 software package and by double-resonance methods with irradiation at 2.88, 2.80, 2.15, 2.08, 1.52 and 1.42 ppm. The geometry of the compounds was optimized using the Avogadro 1.1.1.

1-Hexylcyclopentan-2-one-1-carboxylic acid ethyl ester (1)

Cyclopentan-2-one-1-carboxylic acid ethyl ester (Scheme 1) (99.5 g, 0.637 mol) was dissolved in 350 mL of toluene in a 1 L flask. Sodium metal (14.6 g, 0.637 mol) was then added in small pieces. The mixture was refluxed until achieving the complete dissolution of sodium (for 2 h) and it was then allowed to cool to room temperature. Hexyl bromide (105 g, 0.637 mol) was then added and the resulting mixture was refluxed for 16 h, cooled, washed with water (300 mL), dried over sodium sulphate and evaporated. The residue was distilled under an oil-pump vacuum (at a residual pressure of ~1 mm Hg). Fraction boiling at 160–170 °C was collected. The product was a colourless non-viscous oil. The yield was 75 g (49%). NMR δ H (700 MHz, CDCl₃): 4.27–4.17 (m, 2H), 2.62–2.27 (m, 4H), 2.09–1.92 (m, 3H), 1.65–1.58 (m, 1H), 1.41–1.29 (m, 10H), 0.94 (t, 3H, 7 Hz). δ C (176 MHz, CDCl₃): 214.5, 171.2, 61.3, 60.7, 38.0, 33.9, 32.8, 31.5, 29.6, 24.8, 22.6, 19.6, 14.2, 14.0. ESI MS: [M + Na] 263.1676, calculated 263.1623.

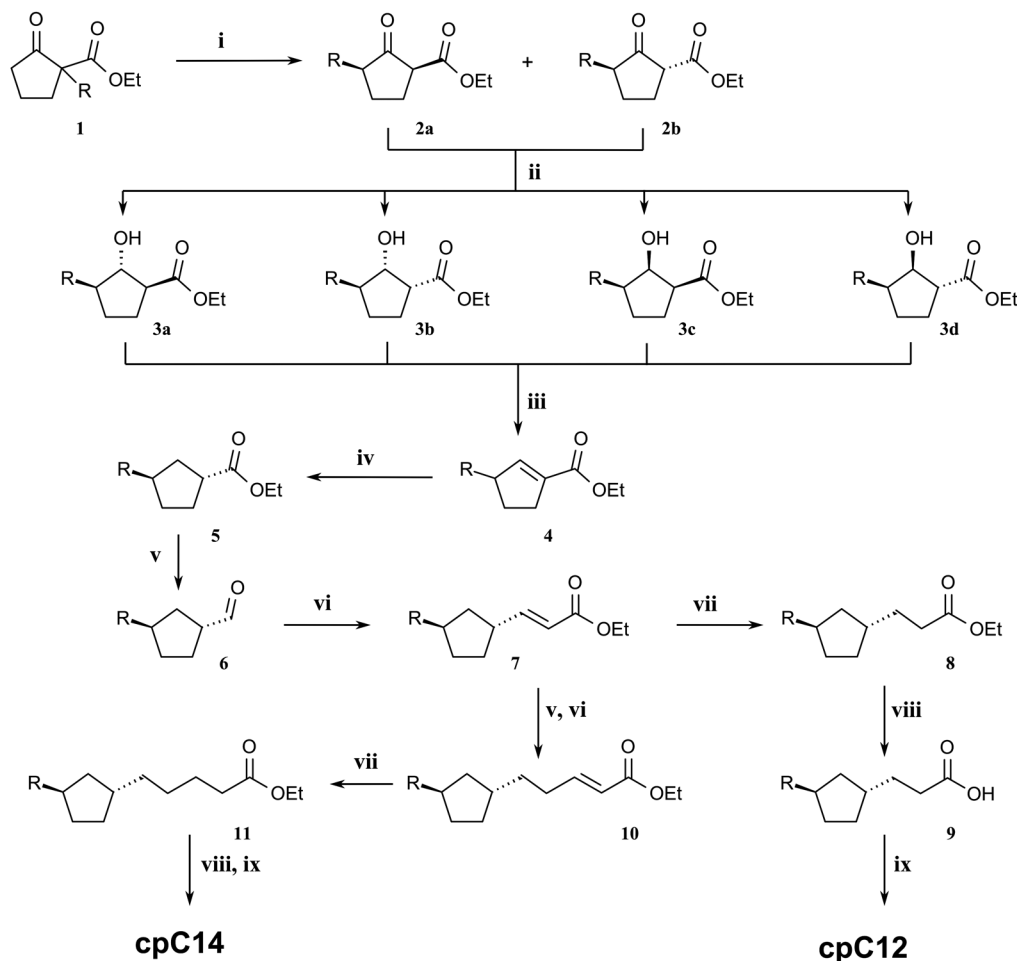
3-Hexylcyclopentan-2-one-1-carboxylic acid ethyl ester (2)

A 250 mL flame-dried flask cooled in argon was charged with 60 mL of dry ethanol (absolute ethanol additionally distilled over sodium ethylate), after which 4.25 g (0.185 mol) of sodium metal was added while stirring. After complete dissolution of sodium, 44.5 g (0.185 mol) of 1-hexyl-cyclopentan-2-one-1-carboxylic acid ethyl ester **1** was added to the flask. The flask was equipped with a reflux condenser with a calcium chloride

tube. The reaction mixture was refluxed for 8 h, after which the reflux condenser was removed, and the flask was equipped for distillation. About 30 mL of alcohol was distilled off. Additional 70 mL of liquid were distilled off after 100 mL of toluene was added into the flask. The residue was allowed to cool to room temperature and then poured into a mixture containing 12 mL of glacial acetic acid and 100 mL of water. The solution was extracted with a toluene–ethyl acetate mixture (1:1, 2 × 150 mL). Organic solutions were combined, dried over sodium sulphate and evaporated. The residue was distilled under an oil-pump vacuum (at a residual pressure of ~1 mm Hg). Fraction boiling at 158–165 °C was collected. The product was a colourless oil. The yield was 29 g (65%). According to NMR analysis, the product was a mixture of two isomers (substituents in the ring were *cis*- or *trans*-oriented). NMR isomer 1: δ H (700 MHz, CDCl₃): 4.30–4.22 (m, 2H, –OCH₂–), 3.17 (dd, 1H, 8 Hz, 11 Hz, cyclopentane C1), 2.38–2.23 (m, 4H, cyclopentane), 1.87–1.78 (m, 1H, 1-hexyl, CH₂), 1.62–1.49 (m, 1H, cyclopentane), 1.45–1.28 (m, 12H, hexyl and ethyl CH₃), 0.94 (t, 3H, 7 Hz, hexyl CH₃); δ C (176 MHz, CDCl₃): 213.1, 169.6, 61.3, 55.1, 49.2, 31.3, 29.7, 29.2, 27.4, 27.3, 25.1, 22.6, 14.1, 14.0. NMR isomer 2: δ H (700 MHz, CDCl₃): 4.30–4.22 (m, 2H, –OCH₂–), 3.30 (dd, 1H, 8 Hz, 5 Hz, cyclopentane C1), 2.43–2.38 (m, 1H, cyclopentane), 2.31–2.13 (m, 3H, cyclopentane), 1.93–1.78 (m, 2H, 1-hexyl CH₂ (1H) and 1H, cyclopentane), 1.45–1.28 (m, 12H, hexyl and ethyl CH₃), 0.94 (t, 3H, 7 Hz, hexyl CH₃); δ C (176 MHz, CDCl₃): 213.9, 169.4, 61.3, 54.3, 48.9, 31.3, 30.0, 29.2, 27.6, 27.4, 25.2, 22.6, 14.1, 14.0; ESI MS: [M + Na] 263.1640, calculated 263.1623.

2-Hydroxy-3-hexylcyclopentane-1-carboxylic acid ethyl ester (3)

Hexylcyclopentan-2-one-1-carboxylic acid ethyl ester (5.7 g, 0.0237 mol) was dissolved in 100 mL of isopropanol. Upon stirring, 2 g of sodium borohydride was added, and the mixture was stirred again until the end of gas evolution. After 15 more



Scheme 1 Synthesis of cpC12 and cpC14. R, hexyl. i, EtONa; ii, NaBH₄; iii, DIAD, PPh₃; iv, H₂ Pd/C; v, DIBAL-H, toluene -70 °C; vi, Ph₃P=CH-COOEt, r.t.; vii, H₂, Pd/C; viii, KOH, H₂O/iPrOH, then 1 N HCl; ix, NaOH, H₂O.

minutes of stirring, the mixture was transferred to a separatory funnel. The reaction flask was rinsed with 100 mL of ethyl acetate and the resulting ethyl acetate solution was also added to the separatory funnel. The combined organic solution was washed twice with 200 mL portions of 5% sodium chloride solution. The organic layer was separated, dried over sodium sulphate and evaporated. The residue was dissolved in chloroform and filtered. Evaporation using a rotary evaporator and drying under high vacuum yielded 5.27 g (92%) of a transparent oil. The oil was further used without additional purification. ESI MS: [M⁺] 242.1825, calculated 242.1882; [M + H] 243.1953, calculated 243.1960; [M + Na] 265.1785, calculated 265.1779.

3-Hexylcyclopent-1-ene-1-carboxylic acid ethyl ester (4)

2-Hydroxy-3-hexylcyclopentan-1-carboxylic acid ethyl ester (5.25 g, 0.0217 mol) and triphenylphosphine (8.65 g, 0.033 mol) were dissolved in dry tetrahydrofuran and cooled to 0 °C in an ice bath. Diisopropyl azodicarboxylate (5.9 mL, 0.0282 mol) was slowly added to the mixture while stirring so that the reaction mixture did not warm above 5 °C. The mixture was then left intact in the ice bath. The ice completely melted in 10 h and the

reaction mixture warmed to room temperature. Upon concentration in a rotary evaporator, the mixture yielded a viscous yellow oil. The oil was mixed with 40 mL petroleum ether having a boiling point of 40–70 °C. Active shaking transformed the mixture of oil and petroleum ether into a yellow solution with a white crystalline precipitate. The precipitate was filtered off and washed with petroleum ether. The organic solutions were combined and evaporated. The residue was purified by chromatography on silica 60 (63–200 μm) using petroleum ether to a petroleum ether–chloroform (1 : 1) gradient. Evaporation of fractions yielded 3.3 g (67%) of a colourless transparent non-viscous oil. NMR δ H (700 MHz, CDCl₃): 6.77 (d, 1H, 1.7 Hz, cyclopentene C2 (CH=C)), 4.28–4.23 (m, 2H, CH₂, ethyl), 2.88–2.81 (m, 1H, cyclopentene C3), 2.70–2.62 (m, 1H, cyclopentene C5b), 2.60–2.53 (m, 1H, cyclopentene C5a), 2.23–2.17 (m, 1H, cyclopentene C4a), 1.63–1.56 (m, 1H, cyclopentene C4b), 1.55–1.48 (m, 1H, 1-hexyl CH₂), 1.43–1.38 (m, 1H, 1-hexyl CH₂), 1.4–1.3 (m, 14H, hexyl and ethyl CH₃), 0.95 (t, 3H, 7 Hz, hexyl CH₃). δ C (176 MHz, CDCl₃): 165.7, 147.5, 135.9, 60.1, 46.4, 35.0, 31.8, 30.9, 30.1, 29.4, 27.8, 22.7, 14.4, 14.1. ESI MS: [M⁺] 224.1746, calculated 224.1776; [M + H] 225.1856, calculated 225.1854.

3-Hexylcyclopentane-1-carboxylic acid ethyl and methyl esters (5)

Hexylcyclopent-1-ene-1-carboxylic acid ethyl ester (1.33 g, 5.93 mmol) was mixed with 60 mg of 10% Pd/C, after which 5 mL of methanol was added and the reaction flask was connected to a hydrogen-filled balloon. The mixture was stirred for 2 days. Over this period, the double bond became completely reduced while the ethyl ester partially transformed into the methyl ester. The reaction was monitored by GC. Upon the completion of the reaction, the solution was filtered through kieselgur and evaporated. The product (1.32 g, 98%) was a colourless transparent oil. According to NMR analysis, it was a mixture of ethyl and methyl esters of 3-hexyl-cyclopentan-1-carboxylic acid. The analysis data presented below indicate that the methyl ester is the main component (more than 90%) of the mixture. NMR δ H (700 MHz, CDCl₃): 3.73 (s, 3H, COOCH₃), 2.84–2.78 (m, 1H, cyclopentane C1), 2.17–2.11 (m, 1H, cyclopentane C2a), 1.98–1.81 (m, 4H, cyclopentane C3, C4a, C5), 1.44–1.38 (m, 3H, 1-hexyl CH₂, cyclopentane C2b), 1.38–1.28 (m, 9H, hexyl CH₂, cyclopentane C4b), 0.94 (t, 3H, 7 Hz). δ C (176 MHz, CDCl₃): 177.2, 51.5, 43.7, 40.7, 37.1, 35.7, 32.0, 31.9, 29.6, 28.9, 28.6, 22.7, 14.1. ESI MS: [M + H] 227.2020, calculated 227.2011; [M + Na] 249.1849, calculated 249.1830.

3-Hexylcyclopentane-1-carboxaldehyde (6)

Solution of compound 5 (1.07 g, 5 mmol) in 12 mL of dry toluene was sealed and cooled in an acetone/liquid nitrogen bath. A 1 N DIBAL-H solution in cyclohexane (7.5 mL) was slowly injected through a septum. After 3 h, 6 mL of methanol was injected and the mixture was kept in the bath for 30 more minutes. The mixture was then poured into 50 mL of ethyl acetate and washed with a 10% K, Na tartrate solution (4 × 50 mL) and with water (2 × 50 mL). The organic layer was dried over Na₂SO₄ and evaporated. Chromatography was performed on silica 60 using a CHCl₃–petroleum ether mixture (1 : 1) as an eluent and, as the result, 565 mg (62%) of compound 6 was obtained as a colourless transparent oil. NMR δ H (700 MHz, CDCl₃) (1,3-*trans* isomer) 9.67 (d, 2.6 Hz, 1H, CHO), 2.84–2.78 (m, 1H, >CH–CHO, cyclopentane), 2.1–2.04 (m, 1H, C(2)Ha, cyclopentane), 2.02–1.81 (m, 4H, [1.99, C(5)Ha; 1.96, C(3)H; 1.90, C(4)Ha; 1.85, C(5)Hb]), 1.45–1.30 (m, 11H, CH₂ alkyl + C(2)Hb cyclopentane), 1.26–1.19 (m, 1H, C(4)Hb, cyclopentane), 0.96 (t, 6.9 Hz, CH₃). δ C (176 MHz, CDCl₃): 204.1, 51.5, 40.7, 35.5, 33.3, 32.2, 31.8, 29.5, 28.6, 25.7, 22.6, 14.0. ESI MS: [M + H] 183.1753, calculated 183.1749.

3-(3-Hexylcyclopentyl)-2-propenoic acid ethyl ester (7)

A solution of aldehyde 6 (907 mg, 4.98 mmol) in toluene was treated with 2.6 g (7.46 mmol) of ethyl (triphenylphosphoranylidene)acetate. The mixture was shaken to dissolve all the materials and left overnight. Olefin 7 (a colourless transparent oil, 1.07 g, 85%) was isolated by chromatography on silica 60 using a CHCl₃–petroleum ether mixture (1 : 1) as an eluent. NMR δ H (700 MHz, CDCl₃) (1,3-*trans* isomer) 7.00 (dd, 15.6 7.9 Hz, 1H, CH=CH–COO), 5.84 (d, 15.6 Hz, 1H, CH–COO), 4.25 (q, 7.2 Hz, 2H, O–CH₂), 2.72–2.65 (m, 1H, C(1)H, cyclopentane),

2.08–1.85 (m, 4H, cyclopentane), 1.58–1.51 (m, 1H, cyclopentane), 1.43–1.29 (m, 14H [10H CH₂ alkyl, 1H CH cyclopentane, 3H –CH₂–CH₃]), 1.10–1.03 (m, 1H, cyclopentane), 0.95 (t, 7.1 Hz, CH₃). δ C (176 MHz, CDCl₃): 167.0, 153.8, 119.4, 60.17, 42.89, 40.37, 40.00, 36.38, 31.98, 31.76, 31.34, 29.6, 28.68, 22.73, 14.39, 14.16. ESI MS: [M + H] 253.2172, calculated 253.2167.

3-(3-Hexylcyclopentyl)-propanoic acid ethyl ester (8) and 3-(3-hexylcyclopentyl)-propanoic acid (9)

In a flask connected to hydrogen (1.2 atm), 570 mg (2.26 mmol) of 3-(3-hexylcyclopentyl)-2-propenoic acid ethyl ester, 80 mg Pd/C, and 10 mL of methanol were mixed together and stirred for 5 h. The solution was then filtered and evaporated. The product, a colourless transparent oil (560 mg), was mixed with a KOH solution in a 2 : 5 water–iPrOH mixture (200 mg, 7 mL) and left overnight. The solution was evaporated (ethanol was added when needed to reduce foaming), neutralized with 1 N HCl and extracted with ether. The ether solution was washed with water and evaporated yielding a colourless oil (500 mg, 91%). NMR (3-(3-hexylcyclopentyl)-propanoic acid) δ H (700 MHz, CDCl₃) (1,3-*trans* isomer) 2.44–2.40 (m, 2H, CH₂COO), 2.04–1.78 (m, 5H, cyclopentane [2.00, 1H, C(2)Ha; 1.89, 1H, C(1)H; 1.86, 1H, C(3)H; 1.82, 1H, C(5)Ha; 1.81, 1H, C(4)Ha]), 1.75–1.68 (m, 2H, CH₂CH₂COO), 1.39–1.29 (10H, CH₂ alkyl), 1.29–1.22 (m, 2H [1H, C(4)Hb; 1H C(5)Hb]), 0.95 (t, 7.4 Hz, 3H, CH₃), 0.77–0.71 (m, 1H, C(2)Hb, cyclopentane). δ C (176 MHz, CDCl₃): 179.5, 40.3, 40.2, 39.6, 36.6, 33.2, 31.9, 31.6, 31.4, 31.3, 29.6, 28.7, 22.7, 14.1. ESI MS: [M + H] 227.2007, calculated 227.2011.

3-(3-Hexylcyclopentyl)-2-pentenoic acid ethyl ester (10) was obtained as described for compound 7, starting from compound 8 instead of compound 5. NMR δ H (700 MHz, CDCl₃) (1,3-*trans* isomer) 7.04 (dd, 15.5 7.89 Hz, 1H, CH=CH–COO), 5.88 (d, 15.5 Hz, 1H, CH–COO), 4.26 (q, 7.2 Hz, 2H, O–CH₂), 2.28–2.23 (m, 2H, CH₂–CH=), 2.02–1.97 (m, 1H, cyclopentane), 1.91–1.83 (m, 2H, cyclopentane), 1.82–1.78 (m, 2H, cyclopentane), 1.55–1.48 (m, 2H, CH₂–CH₂–CH=), 1.38–1.29 (m, 13H, 10H alkyl, 3H CH₃–CH₂–O), 1.26–1.21 (m, 2H, cyclopentane), 0.95 (t, 7.1 Hz, CH₃), 0.76–0.70 (m, 1H, cyclopentane). δ C (176 MHz, CDCl₃): 166.8, 149.7, 121.2, 60.1, 40.5, 40.2, 39.6, 36.7, 34.9, 31.9, 31.6, 31.5, 31.4, 29.6, 28.7, 22.7, 14.3, 14.1. ESI MS: [M + H] 282.2563, calculated 282.2558.

3-(3-Hexylcyclopentyl)-2-pentanoic acid ethyl ester (11) and 3-(3-hexylcyclopentyl)-2-pentanoic acid (12) were obtained as described for compounds 8 and 9, starting from 10 instead of compound 7. NMR (3-(3-hexylcyclopentyl)-2-pentanoic acid) δ H (700 MHz, CDCl₃) 2.44–2.40 (m, 2H, CH₂COO), 1.94–1.88 (m, 1H, cyclopentane), 1.87–1.68 (m, 4H, cyclopentane), 1.76–1.67 (m, 2H, CH₂CH₂COO), 1.37–1.21 (14H, CH₂ alkyl), 1.19–1.11 (m, 2H, cyclopentane), 0.87 (t, 7.4 Hz, 3H, CH₃), 0.67–0.61 (m, 1H, cyclopentane). ESI MS: [M + H] 254.2239, calculated 254.2245.

cpC12 and cpC14 were obtained by mixing 3-(3-hexylcyclopentyl)-propanoic acid 9 or 3-(3-hexylcyclopentyl)-2-pentanoic acid 12 with equimolar amounts of 1 N NaOH followed by

careful vortexing until clean. The solution was evaporated. To reduce foaming, ethanol was at times added. The residue was vacuum dried to yield a white powder.

CMC and Krafft point

Theoretical prediction. Both cyclopentane-containing and common surfactants have the same polar heads and the difference in packing is determined exclusively by hydrophobic tails. Thus, polar heads are excluded from the consideration.

If melting temperature is the point of equilibrium between ordered and disordered phases, it demands the equality of the Gibbs free energies of both phases. The Gibbs free energy of the system is given by the well-known equation

$$G = H - TS, \quad (1)$$

where H is the enthalpy, T is the temperature, and S is the entropy of the system. We can express the critical temperature T_c (the melting temperature) in terms of enthalpy and entropy:

$$T_c = \frac{H_{\text{dis}} - H_{\text{ord}}}{S_{\text{dis}} - S_{\text{ord}}}. \quad (2)$$

Indices ord and dis in this equation refer to the characteristics of the ordered and disordered phases, respectively. The ratio of the critical temperatures for a normal chain (corresponding characteristics are denoted by the index N) and a cyclopentane-containing chain (corresponding characteristics are denoted by the index CP) can be derived from eqn (2):

$$\frac{T_{c,CP}}{T_{c,N}} = \frac{\Delta H_{CP} \Delta S_N}{\Delta H_N \Delta S_{CP}} = \frac{H_{\text{dis},CP} - H_{\text{ord},CP}}{H_{\text{dis},N} - H_{\text{ord},N}} \frac{S_{\text{dis},N} - S_{\text{ord},N}}{S_{\text{dis},CP} - S_{\text{ord},CP}}. \quad (3)$$

The entropy can be estimated by the Boltzmann relation: $S = k \ln(W)$, where W is the number of microstates of a surfactant molecule; k is the Boltzmann constant. We assume each molecular conformation as a microstate. In frames of the model, we define an ordered phase as one in which weak thermal fluctuations can be neglected and there is only one conformation of the surfactant molecule, *i.e.* the all-*trans* conformation (see Fig. 2). The number of states $W_{\text{ord}} = 1$, $S_{\text{ord}} = 0$, and thus the entropy change $\Delta S = S_{\text{dis}}$. Furthermore, we define a disordered state as one in which all possible conformations are implemented. Total number of possible conformations is

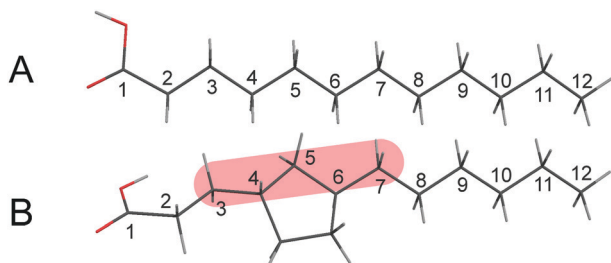


Fig. 2 Conformation of a hydrophobic chain with a cyclopentane fragment compared to that of lauric acid. Structures were obtained by quantum chemistry optimization. (A) All-*trans* lauric acid. (B) Lauric acid with a cyclopentane fragment. Bonds with fixed (frozen) conformation are highlighted.

the number of combinations of *trans/gauche* variants for each segment of a chain.

When evaluating the transition enthalpy, we considered that in the disordering or melting process, the hydrocarbon chains (i) gain the possibility to adopt *gauche* conformations thus rising their energy; (ii) increase interchain distance and lose mutual order, decreasing interaction energy between neighboring chains. Thus, the enthalpy of the chain comes from the chain self-contribution (*trans/gauche* conformations) and interaction with the neighboring molecules. Both constituents are proportional to the number of C–C bonds, *i.e.* chain length. In the disordering or melting process the neighboring chainlets of the CH_2 groups become non-parallel. We assume that the enthalpy is proportional to the length of the CH_2 -only fragments in hydrocarbon tails. This concept is close to the effective chain-length model.²⁴

Thus, the ratio of enthalpies is:

$$\frac{\Delta H_{CP}}{\Delta H_N} = \frac{n_{CP}}{n_N},$$

where n_{CP} is the number of CH_2 groups involved in direct interaction in cyclopentane-containing molecules and n_N in acyclic ones.

CMC determination. Pyrene (Fluka) was used as an environment-sensitive probe.²⁵ Particularly, micelle formation was traced by changes in the intensity ratio of pyrene fluorescence at 384 and 373 nm (FI373/383), which indicates the environment polarity. Optical density of the sample was kept below 0.05 to avoid the inner filter effect. Pyrene concentration was kept constant during the experiment. Absorbance was measured using an SF256 spectrophotometer (LOMO-Fotonika, Russia). Fluorescence measurements were performed using an F4000 spectrometer (Hitachi, Japan). Excitation monochromator was set to 310 nm. Bandwidths were 5 nm each. Quartz cuvettes were used for the measurements.

The data were fitted with a Boltzmann-type sigmoid as described in ref. 26 for ionic surfactants.

Krafft point determination. Samples were prepared by introducing 2 mL of 100 mM solutions of sodium salts of lauric, myristic, palmytic, cpC12 and cpC14 acids into cuvettes equipped with a magnetic stirring bar and a thermocouple. Samples were heated until transparent and cooled slowly using a Yamato-Komatsu C-22A thermostat. Changes of turbidity were visually observed.

Hydrophobic volume and area calculations

Hydrophobic volume and area calculations were performed using the Marvin software, Marvin 17.6.0, ChemAxon (<https://www.chemaxon.com>).

Molecular dynamics

Molecular dynamics (MD) simulations were performed using the GROMACS package, version 5.1.2. Topology and force field parameters for myristic acid (C14), cpC12, and cpC14 were generated based on slipids force field²⁷ as described elsewhere.²¹ Tip3p water model was used.²⁸ MD simulations were carried out

with a 2 fs time step under 3D periodic boundary conditions in a cubic box with a size of $8 \times 8 \times 8$ nm. Two hundred molecules of the studied acids were randomly distributed in the box. The system was then solvated and the necessary counterions were added. The systems were equilibrated by the steepest descent energy minimization followed by a 500 ps MD run in the isothermal–isobaric (*NPT*) ensemble with an isotropic pressure of 1 bar, a constant temperature of 290 K, and a 1 fs time step. Finally, 500 ns production MD runs were carried out in the isothermal–isovolume (*NVT*) ensemble with constant temperature (280 K) for all the systems. The pressure and the temperature were controlled using the V-rescale thermostat²⁹ and the Parrinello–Rahman barostat³⁰ with 1.0 and 0.1 ps relaxation parameters, respectively, and a compressibility of 4.5×10^{-5} bar⁻¹ for the barostat.

To estimate collective behaviour of the studied molecules, we performed simulations for acyclic and cyclopentane-containing surfactants using the temperatures above and below their Krafft points: sodium salt of C14 was simulated at 280 and 340 K; sodium salt of cpC14, at 275 K; and sodium salt of cpC12, at 280 K.

Phase states were studied by analysing intermolecular contacts (pairs of atoms separated by a distance of <0.4 nm). Detergent clusters (groups of molecules connected *via* the atoms of their nonpolar tails), their interactions and atomic-resolution structures were analysed for each frame (in steps of 100 ps). This analysis was performed using the computer programs specially written for this purpose. The phase state of a surfactant was analysed on the basis of intermolecular contact maps. If the distance between heavy atoms from different molecules was less than 0.4 nm, the contact between these atoms was increased by 1. These maps were normalized to the number of surfactant molecules in the system and averaged over a given calculation interval.

Quantum chemistry calculations

Molecular geometries were optimized by the Hartree–Fock method with the def2-SVP basis set. Calculations were carried out using the ORCA software.³¹ Calculation of the number of conformers was performed using the Open Babel software.³²

Results and discussion

Two cyclopentane-containing surfactants—sodium salts of cyclopentane–C12 (cpC12) and cyclopentane–C14 (cpC14) fatty acids (Fig. 1B)—were synthesized.

Krafft point and CMC

The Krafft point and critical micelle concentration (CMC) are the main characteristics of an ionic surfactant. CMC is the concentration of the surfactant above which micelles form and all surfactant molecules added to the system distribute into micelles; at lower concentrations the surfactant is dissolved in water in the form of single molecules. Krafft point is the minimum temperature of micelle formation by a surfactant. It can be determined from the temperature at which the solubility *vs.* temperature curve intersects the CMC *vs.* temperature curve.³³ There is evidence indicating that the Krafft temperature cannot be precisely described by the phase transition concept and the mass action law should be taken into account.³³ A simpler concept of the Krafft point is the melting point of the hydrated solid of the surfactant.^{34–36} However, melting point definition is still valid for large micelles and reasonable for single surfactant solution.³³ We used this latter definition to describe how cyclopentane rings incorporated into the surfactant hydrocarbon chains affected the Krafft temperature and to predict the magnitude of such an effect.

We assumed that crystal-to-micelle transition of cyclopentane surfactants follows the same stages as in the case of the common surfactants (see the thermodynamics formula derivation in the Experimental section). In the solid state, all hydrophobic chains exist in all-*trans* conformation parallel to each other. The conversion of crystals to micelles is not direct. First, the ordered (crystalline) phase should melt (become disordered). Then surfactant molecules leave the solid phase to the solution and form micelles. We considered the first stage as the limiting one.

We used the total number of possible conformations for a hydrocarbon chain (Table 1) to estimate the entropy change ΔS of the crystal-to-micelle transition of a surfactant. Bond conformations of the cyclopentane chain between atoms C3 and C8 (Fig. 2), which is 5 bonds, are fixed leading to an order of magnitude decrease in the number of possible conformations W . Notably, $W(\text{C12})$ and $W(\text{cpC14})$ are equal because these chains have the same number of bonds around which rotation is possible. The same is valid for the comparison of the C10 ($W = 26\,244$) and cpC12 chains.

Change in the enthalpy ΔH of the transition was assumed to be proportional to the number of CH₂ groups in a chain (excluding the cyclopentane fragment). ΔH and ΔS were used to calculate the ratio of the critical temperatures for a normal chain and a cyclopentane-containing chain (see the Experimental section) and therefore estimate the T_c for the cyclopentane-containing

Table 1 Cyclopentane-containing surfactants (Na salts) compared to their normal counterparts

	C12	cpC12	C14	cpC14
Number of possible conformations of the chain W	236 196	26 244	2 125 764	236 196
Chain volume, Å ³	198.02	220.25	231.94	254.09
Hydrophobic surface area, Å ²	354.19	385.01	415.36	445.43
CMC, mmol	27.5	17.2	7.2	2.7
Krafft point, °C	23.2	−5.0	38.9	6.9
T_c , °C (predicted Krafft point)		−11.2		9.6

chains. Resulting values are reported in Table 1 along with the experimentally measured ones. Even this simple model yields T_c values that are in good agreement with the experimental data.

For normal-chain surfactants, the longer the chain is, the lower the CMC is (Fig. 3B). Sodium salts of cpC12 and cpC14 were found to have a lower CMC than salts of the corresponding acyclic fatty acids; the effect is more pronounced for cpC14 (Fig. 3B and Table 1). We propose that in a more general case, which includes branched or cyclopentane-containing surfactants, CMC rather depends on the volume (or surface area) of the hydrophobic tail than on its length. This approach puts cpC12 and cpC14 in line with the normal-chain surfactants (Fig. 3C and D).

Longer surfactant tails tend to decrease solubility of a surfactant in water and increase its Krafft point. Incorporation of the cyclopentane fragment into a hydrophobic chain decreases the Krafft point considerably. What is more important, is that it provides for better solubilization and lower working concentrations of the surfactants.

Molecular dynamics

Comparison of three surfactants (sodium salts of myristic, cpC12 and cpC14 acids) during their relaxation in water made it possible to identify similarities and differences in their behaviour. All the compounds, which were distributed in the solvent uniformly in the initial configuration, formed aggregates of about 50 molecules during the MD simulations. Moving randomly in the solvent, the micelles interact with each other. Surfactant precipitation is caused by association of these micelles. In aggregates and associates of aggregates, the electrostatic repulsion caused by exposure of negatively charged polar head groups of surfactants to water is neutralized by sodium ions.

Morphologies of aggregate associates produced in the course of the simulations depend on the nature of the surfactant. At a temperature of 280 K, micelles of sodium myristate form a stack of bilayer-like structures (lamellae) (their formation was unrestricted by the periodic boundary conditions) (Fig. 4A). In the lamellae, atoms of myristoyl chain align to form the extended conformation of the chain. Thus, sodium

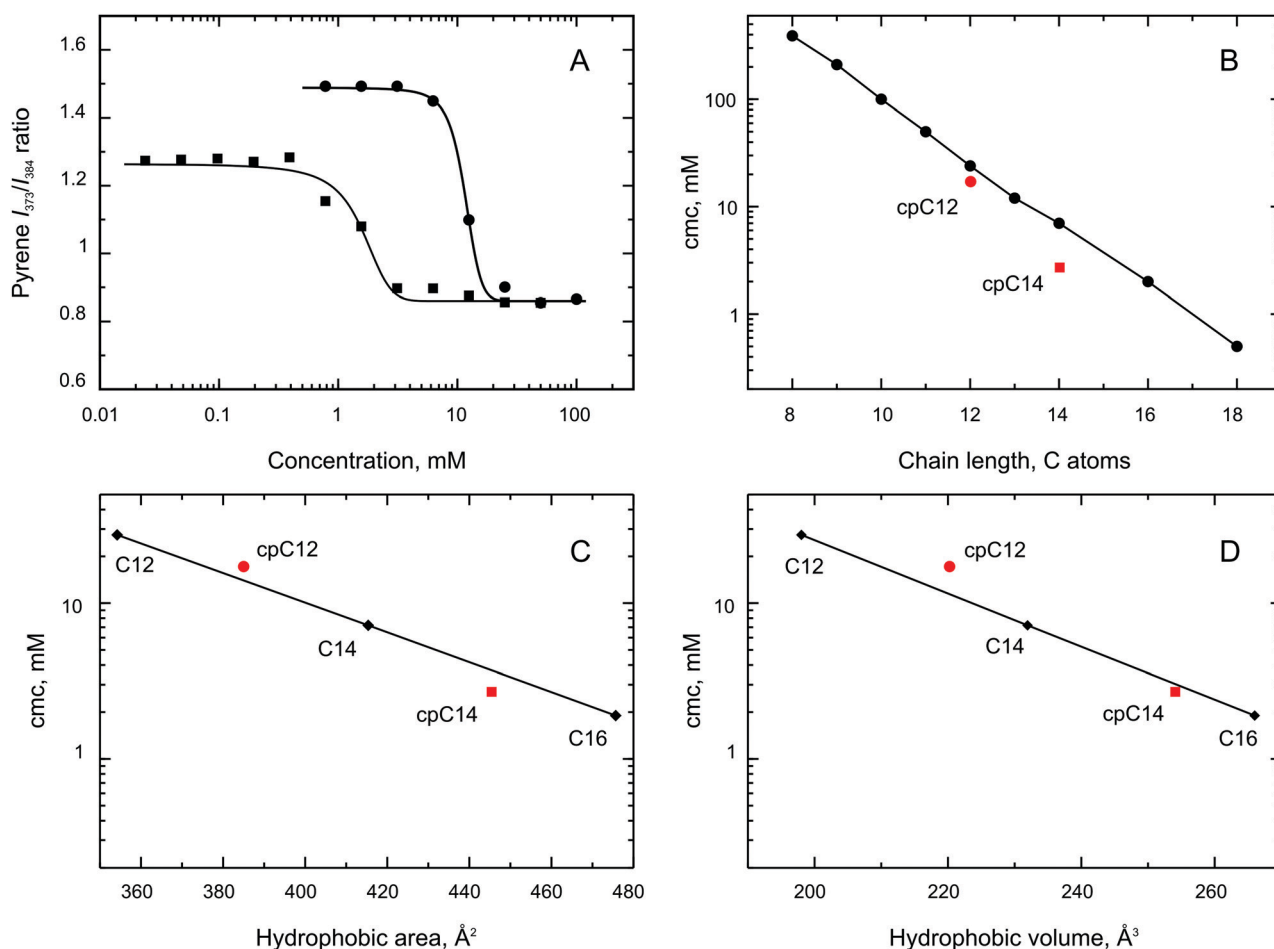


Fig. 3 (A) Determination of the CMC using pyrene fluorescence. Circles represent data for cpC12; squares, for cpC14. Lines represent data fit by a Boltzmann-type sigmoid. (B) CMC vs. the chain length for sodium salts of fatty acids. Red circle and square represent experimental values for cpC12 and cpC14, respectively. (C) CMC vs. hydrophobic surface area of the chain for sodium salts of fatty acids. (D) CMC vs. the hydrophobic volume of the chain for sodium salts of fatty acids.

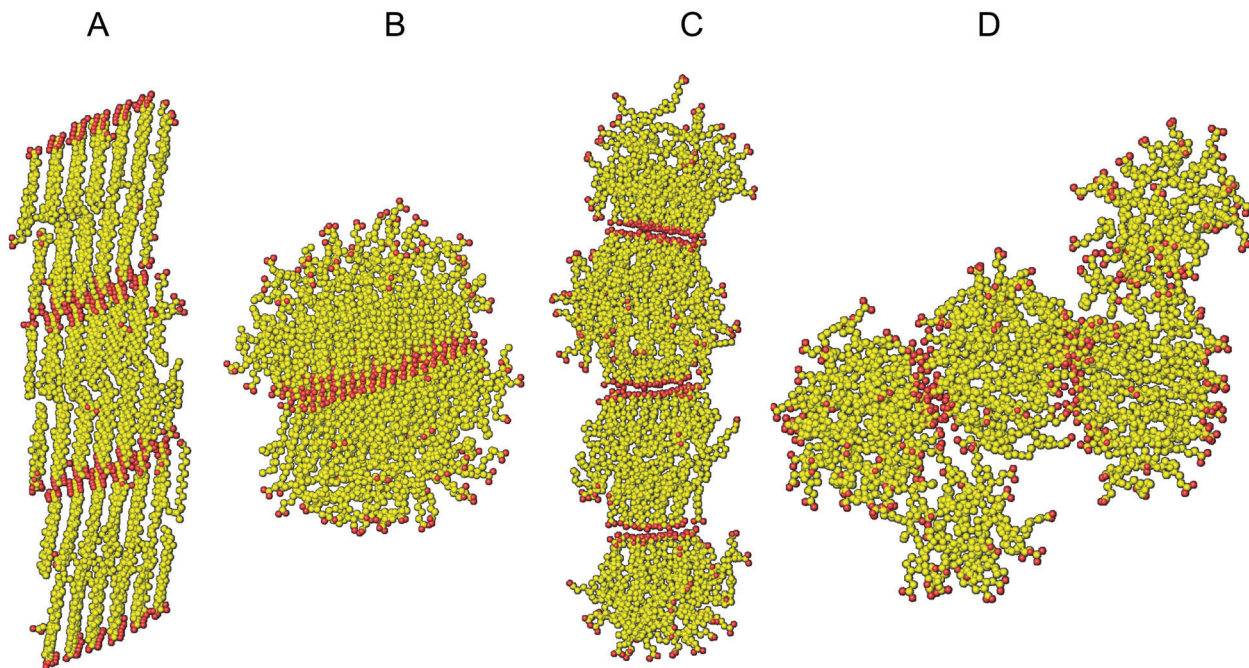


Fig. 4 MD simulation results for water mixtures of sodium myristate, cpC12, and cpC14. Configurations of the following systems were obtained after a 500 ns relaxation: sodium myristate (A) below (280 K) and (B) above (340 K) the Krafft point; cpC14 below the Krafft point (275 K) (C); and cpC12 above the Krafft point (280 K) (D). Yellow and red spheres show the location of carbon and oxygen atoms, respectively. Water molecules, ions, and hydrogen atoms are hidden for simplicity.

myristate behaves like a gel and forms crystals with triclinic $P1$ symmetry.³⁷ The crystal structure is formed in the contact region by charged heads and ions. The formation of such structures is enthalpically favourable. The unfavourable factor is that the entropy of the system decreases with the formation of the gel phase. The latter factor becomes predominant at high temperatures. The behaviour of the system changes when its temperature exceeds the Krafft point. In this case, all sodium myristate molecules form a single cluster—a double micelle—after a 500 ns MD simulation (Fig. 4B). This micelle can be divided into two parts connected *via* polar heads. Carbon tails of the molecules at the contact side of the cluster mostly have extended conformations, whereas molecules at the opposite side of the cluster have curved tails and their polar heads are uniformly distributed over the surface. The formation of a double micelle instead of individual micelles could be a direct consequence of a very high (0.8 M) concentration of the surfactant in the simulation box.

Cyclopentane-containing molecules form a suspension of spherically symmetric micelles (Fig. 4C and D). We were unable to model cpC12 surfactant below T_c since the T_c is below 0 °C and the MD of aqueous solutions in this case could produce artefacts. cpC14 molecules do not form a crystalline phase as normal C14 does below T_c . Formation of the gel phase is hindered for cyclopentane-containing surfactants. However, relatively long hydrophobic chains of the cpC14 molecules make it possible to partially order the hydrocarbon tails, despite the presence of cyclopentane. This, in turn, leads to the ordering of the head region. These micelles can interact with each other, but due to the

lower ability of cyclopentane-containing chains to order (compared to the normal chains), the contact area is smaller, which does not yield double micelles, but chains of smaller sized micelles. Thus, cpC14 below the Krafft point forms chains of micelles similar to those of sodium myristate (Fig. 4C). At temperatures above T_c , micelles tended to move independently as is exemplified by cpC12 micelles in Fig. 4D.

Conclusions

The incorporation of cyclopentanes, which are a distinctive feature of archaeal lipids, into hydrophobic chains of acyclic surfactants imparts these surfactants with the unique properties of the parent compounds. The operational range of cyclopentane-containing surfactants notably expands into the low-temperature region. Unlike acyclic surfactants, cyclopentane-containing surfactants do not form a crystalline phase below the Krafft point; in contrast, their precipitation is caused by the fact that their solubility decreases with temperature.

Conflicts of interest

There are no conflicts to declare.

Acknowledgements

The work was supported by the Russian Science Foundation (project #17-79-20440). NMR experiments were carried out

using the equipment provided by the IBCH core facility (CKP IBCH, supported by the Russian Ministry of Education and Science, grant RFMEFI62117X0018). I. B. designed the study and performed the synthesis, K. M. investigated the *cis-trans* isomers and performed the NMR analysis, M. B. performed the MS analysis, P. V. performed molecular dynamics simulations, I. B. performed quantum chemistry calculations, A. A. and D. T. performed the CMC and Krafft point measurements, and T. G. and I. B. performed theoretical investigations. All the authors contributed to data analysis and manuscript writing.

References

- 1 C. Martinez-Bussenius, C. Navarro and C. Jerez, *Microb. Biotechnol.*, 2017, **10**, 279–295.
- 2 P. R. Norris, *Miner. Eng.*, 2017, **106**, 13–17.
- 3 N. Shrestha, G. Chillkoo, B. Vemuri, N. Rathinam and R. K. Sani, *Bioresour. Technol.*, 2018, **255**, 318–330.
- 4 H. Kurt, M. Özgür, M. Kumru and A. Tunga, *Desalin. Water Treat.*, 2017, **97**, 21598.
- 5 F. Enzmann, F. Mayer, M. Rother and D. Holtmann, *AMB Express*, 2018, 1–22.
- 6 M. A. Amoozegar, M. Siroosi, S. Atashgahi, H. Smidt and A. Ventosa, *Microbiology*, 2017, 623–645.
- 7 J. A. Littlechild, *Archaea*, 2015, **2015**, 1–11.
- 8 E. Bonch-Osmolovskaya and H. Atomi, *Curr. Opin. Microbiol.*, 2015, **25**, vii–viii.
- 9 M. Vogel, S. Matys, F. Lehmann, B. Drobot, T. Gunther, K. Pollmann and J. Raff, *Solid State Phenom.*, 2017, **262**, 389–393.
- 10 D. Farci, F. Esposito, S. El and D. Piano, *Food Res. Int.*, 2017, **99**, 868–876.
- 11 I. Papapetridis, M. Van Dijk, A. J. A. Van Maris and J. T. Pronk, *Biotechnol. Biofuels*, 2017, 1–14.
- 12 P. M. Oger and A. Cario, *Biophys. Chem.*, 2013, **183**, 42–56.
- 13 T. Koyanagi, G. Leriche, D. Onofrei, G. P. Holland, M. Mayer and J. Yang, *Angew. Chem., Int. Ed.*, 2016, **55**, 1890–1893.
- 14 N. Terme, A. Jacquemet, T. Benvegnu, V. Vié and L. Lemiègre, *Chem. Phys. Lipids*, 2014, **183**, 9–17.
- 15 P. V. Panov, S. A. Akimov and O. V. Batishchev, *Biochem. Suppl. Ser. A: Membr. Cell Biol.*, 2014, **8**, 331–335.
- 16 M. Brard, W. Richter, T. Benvegnu and D. Plusquellec, *J. Am. Chem. Soc.*, 2004, **126**, 10003–10012.
- 17 E. Montenegro, B. Gabler, G. Paradies, M. Seemann and G. Helmchen, *Angew. Chem., Int. Ed.*, 2003, **42**, 2419–2421.
- 18 A. Jacquemet, C. Meriadec, L. Lemiegre, F. Artzner and T. Benvegnu, *Langmuir*, 2012, 7591–7597.
- 19 A. Jacquemet, L. Lemierge, O. Lambert and T. Benvegnu, *J. Org. Chem.*, 2011, **76**, 9738–9747.
- 20 P. L. Chong, U. Ayesa, V. P. Daswani and E. C. Hur, *Archaea*, 2012, **2012**, 138439.
- 21 A. O. Chugunov, P. E. Volynsky, N. A. Krylov, I. A. Boldyrev and R. G. Efremov, *Sci. Rep.*, 2014, **4**, 1–8.
- 22 R. D. Boyer, R. Johnson and K. Krishnamurthy, *J. Magn. Reson.*, 2003, **165**, 253–259.
- 23 M. J. Thrippleton and J. Keeler, *Angew. Chem., Int. Ed.*, 2003, **42**, 3938–3941.
- 24 G. Cevc, *Biochemistry*, 1991, **30**, 7186–7193.
- 25 A. A. Semenova, A. O. Chugunov, P. V. Dubovskii, V. V. Chupin, P. E. Volynsky and I. A. Boldyrev, *Chem. Phys. Lipids*, 2012, **165**, 382–386.
- 26 J. Aguiar, P. Carpena and C. C. Ruiz, *J. Colloid Interface Sci.*, 2003, **258**, 116–122.
- 27 I. Ermilova and A. P. Lyubartsev, *J. Phys. Chem. B*, 2016, **120**, 12826–12842.
- 28 W. L. Jorgensen, J. Chandrasekhar, J. D. Madura, R. W. Impey and M. L. Klein, *J. Chem. Phys.*, 1983, **926**, 926–935.
- 29 G. Bussi, D. Donadio and M. Parrinello, *J. Chem. Phys.*, 2007, **126**, 014101.
- 30 M. Parrinello and A. Rahman, *J. Appl. Phys.*, 2012, **52**, 7182–7190.
- 31 F. Neese, *Wiley Interdiscip. Rev.: Comput. Mol. Sci.*, 2012, **2**, 73–78.
- 32 N. M. O'Boyle, M. Banck, C. A. James, C. Morley, T. Vandermeersch and G. R. Hutchison, *J. Cheminf.*, 2011, **3**, 33–47.
- 33 Y. Moroi, R. Sugii and R. Matuura, *J. Colloid Interface Sci.*, 1984, **98**, 184–191.
- 34 M. Hato, *J. Phys. Chem.*, 1972, 378–381.
- 35 K. Tsujil and J. Mino, *J. Phys. Chem.*, 1978, **82**, 1610–1614.
- 36 H. Nakayama and K. Shinoda, *J. Phys. Chem.*, 1966, **102**, 3502–3504.
- 37 C. Boehm, F. Leveiller, D. Jackuemain, H. Moehwald, K. Kjaer, J. Als-Nielsen, I. Weissbuch and L. Leiserowitz, *Langmuir*, 1994, **10**, 830–836.